Journal of Cellular Biochemistry 76:463–477 (2000)

Androgen and Taxol Cause Cell Type-Specific Alterations of Centrosome and DNA Organization in Androgen-Responsive LNCaP and Androgen-Independent DU145 Prostate Cancer Cells

Heide Schatten,[1,2]* **Maureen Ripple,**[3,4,6] **Ron Balczon,**[5] **Richard Weindruch,**[3,4] **Amitabha Chakrabarti,**[1] **Meghan Taylor,**[1] **and Christopher N. Hueser**[1,2]

[1]Department of Veterinary Pathobiology, University of Missouri–Columbia, Columbia, Missouri 65211
[2]Cancer Research Center, Columbia, Missouri 65211
[3]Institute on Aging, University of Wisconsin, Madison, Wisconsin 53706
[4]GRECC William S. Middleton Veterans Administration Hospital, Madison, Wisconsin 53792
[5]Department of Structural and Cellular Biology, University of South Alabama, Mobile, Alabama 36688
[6]Department of Medicine, University of Wisconsin Comprehensive Cancer Center, Madison, Wisconsin 53706

Abstract We investigated the effects of androgen and taxol on the androgen-responsive LNCaP and androgen-independent DU145 prostate cancer cell lines. Cells were treated for 48 and 72 h with 0.05–1 nM of the synthetic androgen R1881 and with 100 nM taxol. Treatment of LNCaP cells with 0.05 nM R1881 led to increased cell proliferation, whereas treatment with 1 nM R1881 resulted in inhibited cell division, DNA cycle arrest, and altered centrosome organization. After treatment with 1 nM R1881, chromatin became clustered, nuclear envelopes convoluted, and mitochondria accumulated around the nucleus. Immunofluorescence microscopy with antibodies to centrosomes showed altered centrosome structure. Although centrosomes were closely associated with the nucleus in untreated cells, they dispersed into the cytoplasm after treatment with 1 nM R1881. Microtubules were only faintly detected in 1 nM R1881-treated LNCaP cells. The effects of taxol included microtubule bundling and altered mitochondria morphology, but not DNA organization. As expected, the androgen-independent prostate cancer cell line DU145 was not affected by R1881. Treatment with taxol resulted in bundling of microtubules in both cell lines. Additional taxol effects were seen in DU145 cells with micronucleation of DNA, an indication of apoptosis. Simultaneous treatment with R1881 and taxol had no additional effects on LNCaP or DU145 cells. These results suggest that LNCaP and DU145 prostate cancer cells show differences not only in androgen responsiveness but in sensitivity to taxol as well. J. Cell. Biochem. 76:463–477, 2000.

Key words: cytoskeleton; mitosis; cell proliferation; cell culture; centrosomes

Hormones play a significant role in the regulation of prostate growth during development and in maintaining homeostasis in adult prostate tissue. During puberty and organ development, low concentrations of androgen stimulate cell divisions that result in full development of the prostate. Normal prostate development depends on androgens, and prostate function is maintained in the adult with high serum concentrations of 5α-dihydrotestosterone (DHT). After age 40, serum testosterone levels decrease, producing morphological changes in the prostate and enlargement of the gland [Narayan, 1995; Wilding, 1995].

Prostate cancer is associated with aging and occurs in a latent or clinical form in 30–40% of men by age 30–50, increasing to 75% in men by age 80 [Tanagho et al., 1995; Thompson et al., 1995]. About 75% of tumors in men with meta-

Grant sponsor: NASA; Grant number: NAG10-0224; Grant sponsor: NIH; Grant number: T32 AG0002/3-06; Grant sponsor: Cancer Research Center; Grant sponsor: University of Missouri–Columbia.

*Correspondence to: Heide Schatten, Department of Veterinary Pathobiology, University of Missouri–Columbia, 1600 E. Rollins Street, Columbia, MO 65211. E-mail: schattenh@missouri.edu

Received 11 March 1999; Accepted 2 August 1999

static prostate cancer are androgen dependent at initial diagnosis [Thompson et al., 1995; Wilding, 1995]. Androgen-ablative therapy for metastatic prostate cancer is effective for 60–80% of men, but most men develop androgen-independent disease within 2 years [Bubley and Balk, 1996; Evans et al., 1998]. Complete withdrawal by castration reduces serum testosterone by about 90%, but it does not affect androgen biosynthesis in the adrenal glands; it also induces side effects, including osteoporosis. This finding demonstrates the need for alternative and additional forms of treatment for advanced prostate cancer [Tyrell, 1999].

While androgen ablation is used as first-line therapy, chemotherapy can now be used to induce a remission in many men after failure of androgen ablation [Smith and Pienta, 1999]. Such treatment includes taxol [Schiff and Horwitz, 1980], which has been used to treat patients with progressive metastatic prostate cancer [Roth et al., 1993; Danesi et al., 1995; Pienta and Smith, 1997; Guinan et al., 1998; Lokeshwar, 1999; Petrylak et al., 1999; Smith and Pienta, 1999]. While taxol alone induced apoptosis in PC-3 cells [Danesi et al., 1995], its clinical activity is enhanced by combination with other treatments [Pienta and Smith, 1997; Kreis et al., 1999; Petrylak et al., 1999]. Taxol has also been studied in animal models and produced significant differences in tumor volume when administered in a rat prostate cancer model [Guinan et al., 1998]. The antimetastatic effects of taxol have also been shown in a PC-3 human prostatic tumor variant (PC3-ML), which metastasizes to the lumbar vertebrae in severe combined immunodeficiency-carrying (SCID) mice [Stearns and Wang, 1992]. These studies showed that taxol inhibited secretion of the 72,000-M_r and 92,000-M_r type IV collagenase plus a 57,000-M_r gelatinase and blocked the establishment, growth, and long-term survival of PC-3 ML cells.

Although these studies have contributed significant new information that can be used for the control of prostate cancers, new approaches for multiple drug treatments are being sought to arrest tumor cell growth. Understanding the cellular and molecular mechanisms by which high doses of androgen maintain cell cycle arrest in the adult prostate tissue will contribute to our understanding of how proliferating prostate cancer cells might be induced to reinitiate cell differentiation. This avenue has already been approached in studies using the flavonoid antioxidant silibinin [Zi and Agarwal, 1999]. The studies presented in this article address basic cellular mechanisms that are affected by high doses of androgen and contribute new insights into mechanisms for preventive and treatment strategies for prostate cancer. We investigated the effects of synthetic androgens and taxol in the androgen-responsive LNCaP and androgen-independent DU145 prostate cancer cell lines. LNCaP is a model for primary tumor cells of the prostate, and DU145 is a model of those that have metastasized into neighboring or developmentally related tissue. The experiments focused on DNA, centrosome, microtubule, and mitochondrial organization in cells treated with low and high doses of androgen and with 100 nM taxol.

MATERIALS AND METHODS

Cell Lines and Culture

The androgen-responsive, androgen receptor-positive LNCaP and androgen-independent DU145 prostate carcinoma cell lines were purchased from the American Type Culture Collection (Rockville, MD) and maintained at 37°C in a 5% CO_2/95% air atmosphere in Dulbecco's modified Eagle's medium (DMEM) supplemented with 5% heat-inactivated fetal bovine serum (FBS) (Life Technologies, Grand Island, NY) plus antibiotics and antimycotics (Sigma Chemical Co., St. Louis, MO). Medium was replaced 24 h after plating with DMEM containing 1% FBS and 4% charcoal-stripped (treated) serum (CSS). After 72–96 h, cells were treated with 0.05 or 1.0 nM R1881 (DuPont-NEN, Boston, MA), 0.1–1,000 nM DHT, vehicle control (ethanol) [Ripple et al., 1997a,b], or 100 nM taxol [Schatten et al., 1982]. R1881 is a synthetic androgen that is experimentally useful because it is not metabolized as rapidly as 5α-DHT [Ripple et al., 1997a,b]. Cells were harvested at various times after treatment. Cells were either analyzed on coverslips for immunofluorescence microscopy and scanning electron microscopy (SEM) or detached by trypsination and resuspended in phosphate-buffered saline (PBS; 10 mM phosphate buffer at pH 7.4, 140 mM NaCl, 2.2 mM KCl) or 0.1 M cacodylate buffer for transmission electron microscopy (TEM).

Measurement of Cell Proliferation

LNCaP and DU145 cells (1,000 or 2,500 per well) were plated in 100 µl DMEM plus 1% FBS/4% CSS per well in 96 well plates [Ripple et al., 1997a,b, 1999]. Experiments were conducted in medium containing 1% FBS and 4% CSS, in order to limit the adverse growth effects encountered with (CSS) that are unrelated to steroid hormone depletion. For example, the growth of androgen-independent DU145 cells is inhibited in medium containing 5% CSS compared with that in 5% FBS; growth in medium containing 1% FBS and 4% CSS is identical to growth in medium containing 5% FBS; this serum mixture is low enough in androgen content to slow the growth of the androgen-responsive LNCaP cells, yet it facilitates detection of an androgen growth response. At 24 or 72 h after plating, the cells were treated in sets of six with 0.001–5 nM R1881 (DuPont-NEN), 0.1–1,000 nM DHT (Sigma), or vehicle control. Control medium contained the ethanol vehicle. Cells were harvested at various times after treatment. The amount of DNA per well was quantitated with a 96-well fluorometric assay [Rago et al., 1990] on a CytoFluorometric plate scanner (PerSeptive Biosystems, Farmington, MA) and analyzed with CytoCalc software (PerSeptive Biosystems, Farmington, MA). The formation of hydrogen peroxide and hydroxyl radical by intact cells was determined by use of a fluorescence probe, 2′,7′-dichlorofluorescein diacetate (DCF) (Molecular Probes, Eugene, OR), as described by Kane et al. [1993]. DCF fluorescent units per well 45 min after addition of DCF were normalized to the DNA fluorescent units of the same well. The data expressed are the average DCF fluorescent units per DNA fluorescent units of six wells ±SD.

Statistical Analysis

Experiments conducted in 96-well plates were done as six replicates. Each treated group was compared with the untreated control by use of the unpaired two-tailored Student's *t*-statistic and tested at the nominal 0.05 significance level. As multiple comparisons were performed, Bonferroni's inequality was implemented for each individual comparison with control for the overall type 1 error rate. For instance, if eight concentrations of androgen were being compared with the control, statistical significance for an individual dose would be determined by a *P*-value of $<0.05/8$ (i.e., $P = 0.00625$). The reported *P*-values reflect the data shown. Only those *P*-values for analyses that are significant after Bonferroni correction are given.

Immunofluorescence Microscopy

For immunofluorescence microscopy, cells were fixed either in methanol for 6 min at −20°C or in 3.7% paraformaldehyde for 10 min [Schatten et al., 1982, 1986] and double- or triple-stained as follows. Centrosomes were stained with either human autoimmune serum 5051 [Calarco-Gillam et al., 1983; Schatten et al., 1986, 1987], autoimmune serum SPJ [Balczon and West, 1991; Schatten et al., 1998a,b], or rabbit polyclonal γ-tubulin antibody (Babco) [Oakley and Oakley, 1989; Stearns and Kirschner, 1994]. Microtubules were stained with either the mouse monoclonal antibody E7 [Schatten et al., 1992; Schatten, 1994] or the rabbit polyclonal antibody generated previously in our laboratory [Bestor and Schatten, 1981]. Incubation in primary antibody for 1 h at 37°C was followed by washes in solution containing 0.1% Triton X-100. The appropriate fluorescein- or rhodamine-labeled anti-mouse, anti-human, or anti-rabbit antibodies were applied for 1 h at 37°C. DNA was fluorescently detected with 10 µM Hoechst 33258 or 2.5% µg/ml DAPI added to the penultimate wash, following the protocols described previously [Schatten et al., 1986, 1987; Schatten, 1994]. Cells were mounted in 90% glycerol in phosphate-buffered saline (PBS) containing 100 µg/ml DABCO (Aldrich) to retard photobleaching. Blind control experiments were performed using second antibody alone to exclude false-positive results. Cells were analyzed using a Zeiss Axiophot microscope equipped with epifluorescence optics.

Scanning Electron Microscopy

Cells were fixed in 2% glutaraldehyde in 0.08 M cacodylic acid, pH 7.4, for 30 min, washed in 0.08% cacodylic buffer for 30 min, and postfixed with 0.1% OsO_4 for 10 min. After washing in distilled water, the preparations were dehydrated through an ethanol series (50%, 70%, 80%, 95%, and 100%) and critical point dried [Ris, 1985]. The samples were imaged with a JEOL JSM-35 scanning electron microscope after metal coating with a thin layer of platinum.

Transmission Electron Microscopy

For TEM, cells were fixed in 2% glutaraldehyde in 0.08 M cacodylic acid, pH 7.4, with

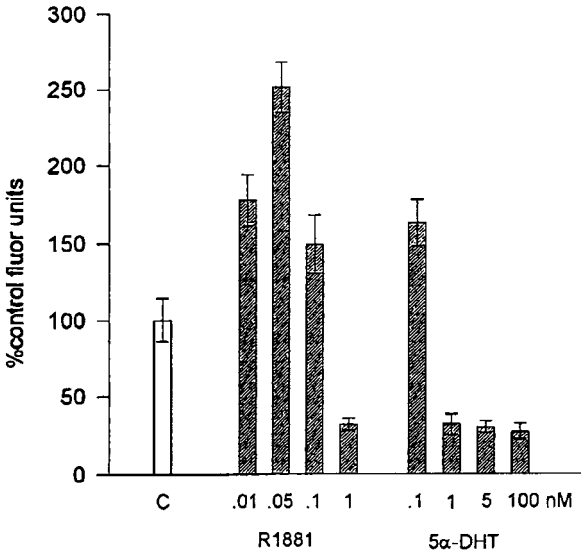

Fig. 1. Dose response of LNCaP cells to the synthetic androgen R1881 and 5α-DHT. LNCaP cells were plated in 96-well plates in Dulbecco's modified Eagle's medium (DMEM) containing 1% fetal bovine serum (FBS) plus 4% charcoal-stripped serum (CSS) (1,000 cells/well). The next day, the cells were treated with media containing R1881, 5α-dihydrotestosterone (5α-DHT), or vehicle control. The plates were harvested and assayed for DNA content 6 days after treatment. Results are expressed as percentage of control fluorescence ± SD (n = 6). R1881 at 0.01 nM stimulates growth above control, while 1 nM inhibits growth. 5α-DHT stimulates growth at 0.1 nM and inhibits growth at 1–100 nM.

0.05% saponin for 30 min. After washes in 0.08 M cacodylic buffer, 10-min postfixation in 0.1% OsO_4 followed. After a series of dehydration, cells were embedded in Epon. Lead- and uranyl-stained sections were analyzed with either a Hitachi H-600 transmission or a JEOL 1200EX scanning/transmission electron microscope.

RESULTS

The dose-dependent effects of R1881 and 5α-DHT on LNCaP cells are shown in Figure 1. Exposure to low concentrations of R1881 (0.01–0.1 nM) stimulates growth above control, while 1 nM inhibits growth. 5α-DHT stimulates growth at 0.1 nM and inhibits growth at 1–100 nM. These results are obtained under growth conditions of LNCaP cells in 96-well plates in DMEM containing 1% FBS plus 4% CSS (1,000 cells/well). Cells were treated with media containing R1881, 5α-DHT, or vehicle control. The plates were harvested and assayed for DNA content at 6 days after treatment. The results are expressed as the percentage of control fluorescence ±SD (n = 6). As expected, under identical experimental conditions, R1881 or 5α-DHT did not appear to have any effect on growth conditions and DNA content in hormone-independent DU145 cells (Fig. 2).

Growth-stimulated LNCaP cells and DU145 cells treated with R1881 exhibited normal phenotypes, whereas LNCaP cells treated with 1 nM R1881 displayed altered phenotypes. We focused our attention on hormone-inhibited LNCaP cells to determine the cell cycle-specific processes that are inhibited by high concentrations of R1881. In LNCaP cells visualized with SEM, control cells show an elongated rounded appearance (Fig. 3a,b). After 72-h treatment with 1 nM of the synthetic androgen R1881 (Fig. 3c,d), cells are attached to each other in patches and appear flattened. TEM of untreated LNCaP cells shows cells in all stages of the cell cycle (Fig. 4a,b), while 95% of hormone-treated cells (1 nM R1881 for 72 h) were arrested before mitosis with one or two sets of chromatin within the intact nucleus (cell sections, Fig. 4c,d). Other differences seen with TEM include convoluted nuclear envelopes in the hormone-treated cells and smooth round nuclear envelopes in control cells. Mitochondria accumulate around the nucleus in 1 nM R1881-treated cells with twice the number observed in control cells.

Because centrosome and DNA cycles are normally synchronous in a regular cell cycle, we investigated whether centrosome cycles are also arrested or altered in hormone-arrested LNCaP cells. Centrosomes are microtubule organizing centers closely associated with the nucleus during interphase and duplicate during the S phase. Like chromosomes, they separate during mitosis and form the bipolar mitotic apparatus. When centrosomes in LNCaP cells are analyzed with immunofluorescence microscopy using anticentrosome antibodies, including SPJ [Balczon and West, 1991], bright centrosomal staining is detected close to the nuclear envelope in control cells (Fig. 5a). In LNCaP cells treated with 1 nM R1881, centrosome structure dissociates from the nucleus and becomes gradually dispersed in the cytoplasm, as seen at 48 h after hormone treatment (Fig. 5c) and at 72 h after hormone treatment (Fig. 5e). The corresponding DNA stained images are shown in Figure 5b,d,f, respectively. The altered fluorescence staining with the SPJ antibody in hormone-treated LNCaP cells indicates either continued synthesis of centrosome proteins and uncou-

pling of the centrosome cycle from the DNA cycle or dispersion into an uncompacted state of condensation. Staining for microtubules was diminished or absent (data not shown) in LNCaP cells treated with 1 nM R1881; this finding may indicate either that microtubules are necessary for positioning centrosomes to their nuclear location during interphase or that the disrupted centrosomes do not nucleate microtubules efficiently. Growth stimulation of LNCaP cells with low concentrations of R1881 (0.05 nM) did not affect centrosome organization. Centrosomes remain associated with the nucleus and do not disperse within the cytoplasm (Fig. 6a, centrosomes; Fig. 6b, DNA). As expected, hormone treatment did not affect centrosomes in the hormone-independent DU145 cell line (data not shown).

To analyze the cell cycle phases affected by 1 nM R1881 in LNCaP cells, we subjected LNCaP cells to flow cytometry. The cell cycle data suggest a G_2/M block after 72 h of 1 nM R1881 under confluent conditions and a slight but not statistically significant G_0/G_1 block under subconfluent conditions (data not shown).

To test whether the cytoskeletal drug taxol has additional inhibitory effects on hormone-treated LNCaP cells, we treated cells with 1 nM R1881 and 0.1–10 μM taxol. Treatment with 100 nM taxol demonstrated dense microtubule bundling in both LNCaP and DU145 cells. Higher concentrations of taxol did not enhance the effects. Taxol treatment had no effect on DNA organization in LNCaP cells, as judged by immunofluorescence and TEM. By contrast, DNA in DU145 cells showed micronucleation after 48 h of 100 nM taxol treatment. Figure 7a shows a DU145 control cell double-stained for centrosome proteins with the SPJ autoimmune antibody and for DNA with the fluorescent dye DAPI. DU145 cells treated with 100 nM taxol for 72 h were double stained for microtubules (Fig. 7b) and for DNA (Fig. 7c). Intense microtubule bundling is seen in Figure 7b, while multiple micronucleation is seen in Figure 7c. While R1881 does not induce apoptosis in LNCaP cells, taxol induces apoptosis in DU145 cells. These results demonstrate different sensitivities of cells not only to hormones, but to treatment with taxol as well.

We also analyzed the effects of 100 nM taxol on the time course of growth (DNA) effects by flow cytometry for LNCaP and DU145 cells. In DU145 cells, a 50% growth inhibitory effect was noted after 5 days of exposure, compared with vehicle control. In LNCaP cells after 5 days of growth, there was little effect on cells treated with 100 nM taxol alone. When LNCaP cells were treated with a growth stimulatory dose (0.05 nM) of R1881, taxol inhibited growth to 50% of the cells treated with only R1881 (data not shown).

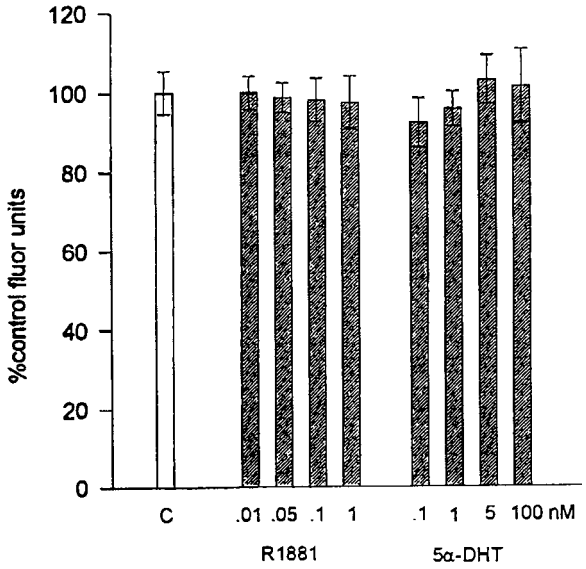

Fig. 2. Dose response of DU145 cells to the synthetic androgen R1881 and 5α-dihydrotestosterone (5α-DHT). DU145 cells were plated in 96-well plates in Dulbecco's modified Eagle's medium (DMEM) containing 1% fetal bovine serum (FBS) plus 4% charcoal-stripped FBS (CSS) (1,000 cells/well). The next day, the cells were treated with media containing R1881, 5α-DHT, or vehicle control. The plates were harvested and assayed for DNA content 6 days after treatment. The results are expressed as percentage of control fluorescence ± SD, (n = 6). R1881 and 5α-DHT have no effect on the growth of DU145 cells.

The typical bundling effects of microtubules in both cell types (LNCaP and DU145) are exhibited by TEM in Figure 8. LNCaP cells (Fig. 8a) display long bundles of microtubules (arrows), while extensive bundling of microtubules (arrows) is shown in Figure 8b for DU145 cells. Differences are also noted in the surface of both cell types. While LNCaP cells have cell surfaces with regular microvilli (open arrows) similar to those seen in untreated LNCaP cells, taxol treatment of DU145 cells causes surface alterations (Fig. 8b, open arrows), which are indications for apoptosis. This supports the finding that DU145 cells are susceptible to apoptosis after taxol treatment. Figure 8c shows morphological mitochondrial alterations in taxol-treated DU145 cells, additional indica-

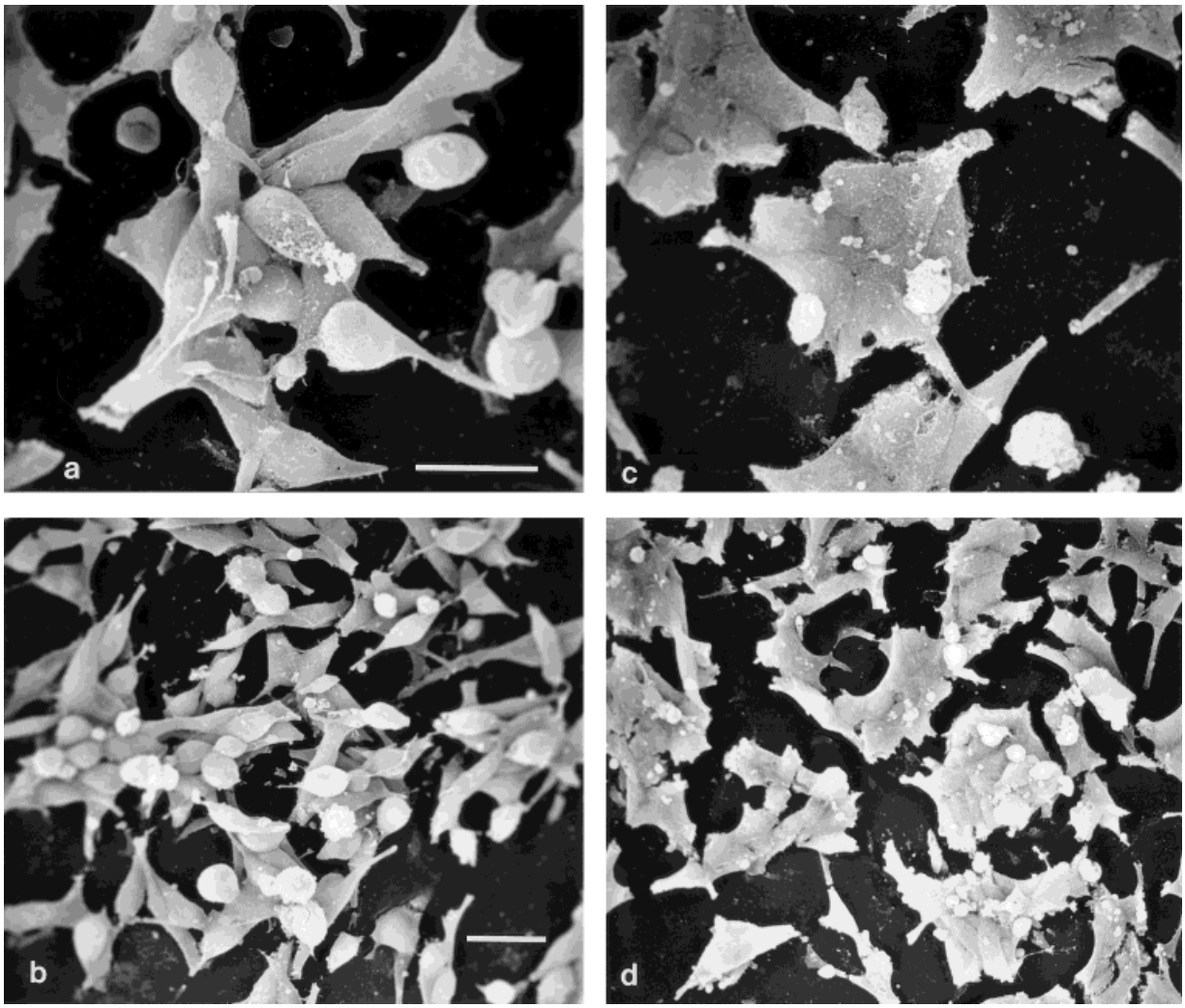

Fig. 3. Scanning electron micrographs of LNCaP cells under normal culture conditions (**a,b**) and when treated with 1 nM of the synthetic androgen R1881 for 72 h (**c,d**). While control cells have an elongated and rounded appearance, hormone-treated cells appear flatter and more attached to each other. Scale bars = 10 μm.

tions for apoptosis in DU145 cells. LNCaP cells do not display apoptotic features.

DISCUSSION

The present study reports effects of hormones and taxol on cell cycle events, focusing on chromosomes and centrosomes in the androgen-responsive LNCaP- and androgen-independent DU145 prostate cancer cells. Hormone therapy and taxol are two treatments available for prostate cancer that are used to inhibit cell division and abnormal tissue growth. Hormones play a significant role during cell cycle regulation in LNCaP cells and in age-related prostate cancer [Ripple et al., 1997a,b], whereas taxol is used to prevent cell division in a variety of different cell types [Schiff and Horwitz, 1980; Schatten et al., 1982]. To investigate the mechanisms of hormone and taxol during cell cycle arrest, we used hormone-responsive prostate cancer cells (LNCaP) and those that have developed hormone independence (DU145).

We found cell cycle arrest in LNCaP cells with high doses of androgen (1 nM R1881) treatment corresponding to physiological levels before age 40, while low concentrations of andro-

Fig. 4. Transmission electron micrographs of untreated LNCaP cells shown in various stages of the cell cycle (**a,** interphase; **b,** mitosis), while 95% of hormone-treated cells (1 nM R1881 for 72 h) are arrested with characteristic two sets of chromatin within the intact nucleus (**c,d**). Note dense accumulation of mitochondria around the convoluted nucleus, not seen in control cells. Scale bar (**a,b**) = 5 μm. Scale bar (**c,d**) = 1 μm.

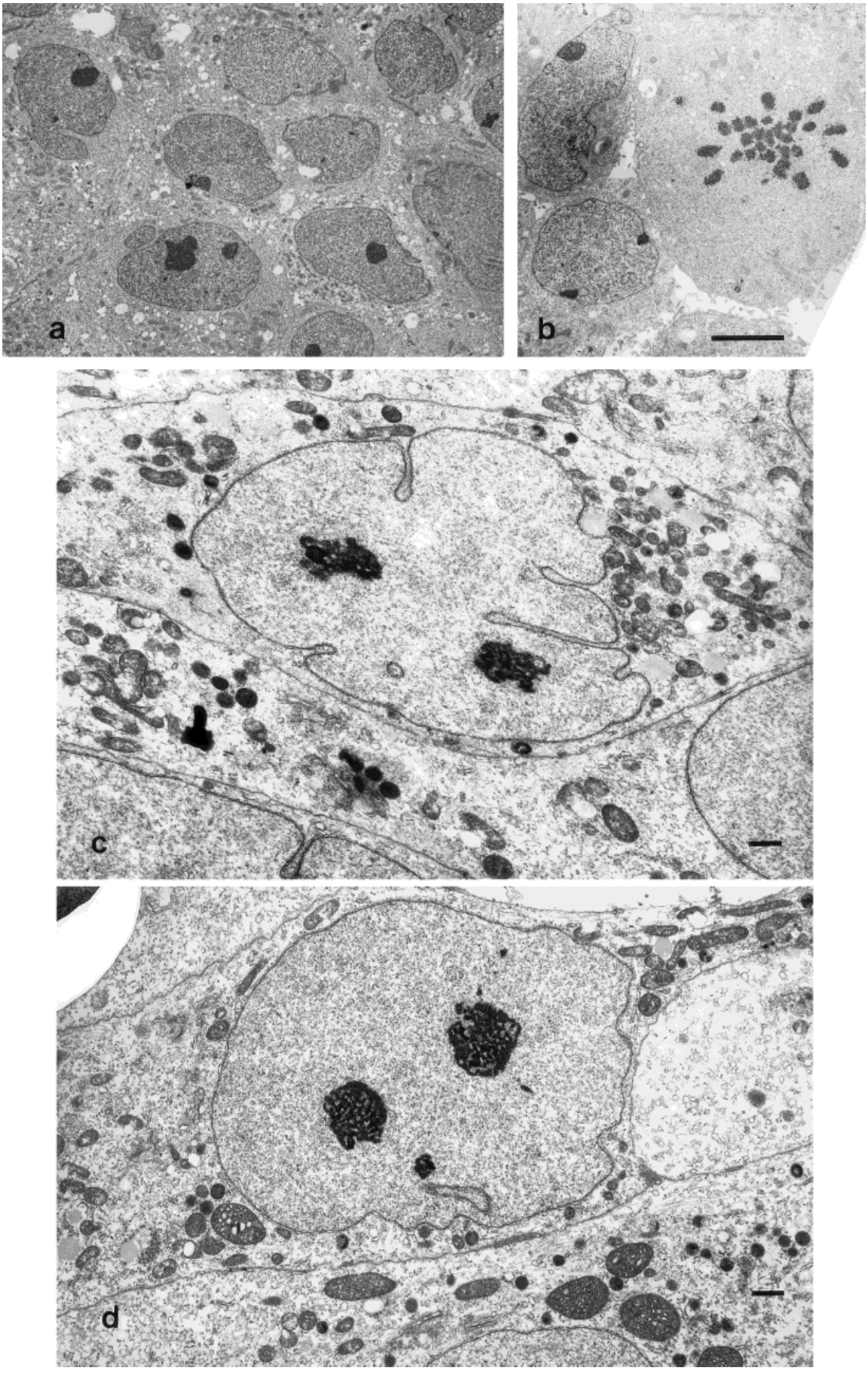

Figure 4.

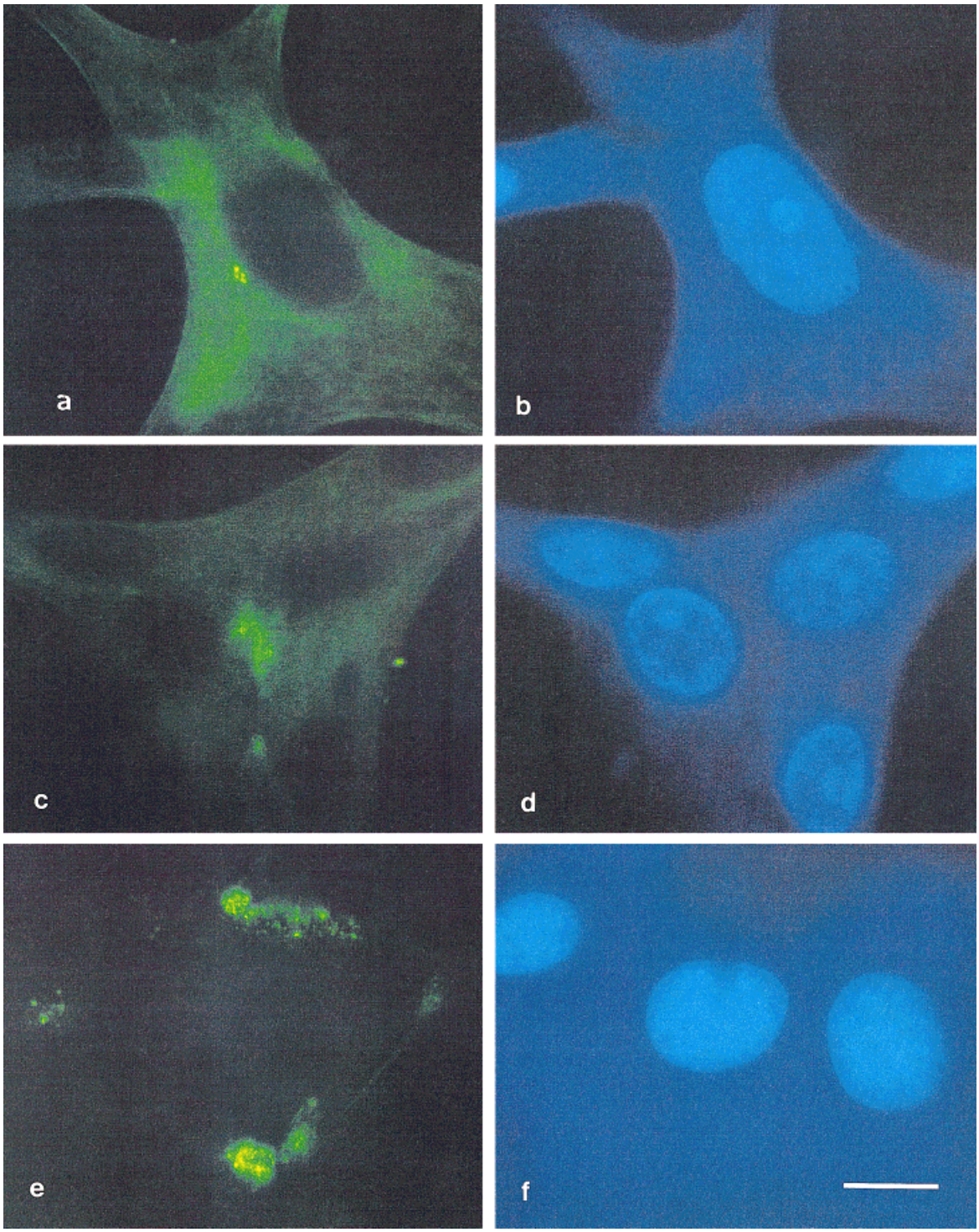

Fig. 5. Immunofluorescence micrographs of centrosomes in LNCaP cells stained with the human autoimmune antibody SPJ show typical centrosomes closely associated with the nucleus in control cells (**a**), while centrosome structure dissociates from the nucleus in hormone-treated (1 nM of the synthetic androgen R1881) cells, gradually accumulating in the cytoplasm as seen at 48 h after hormone treatment (**c**) and at 72 h after hormone treatment (**e**). Corresponding images for nuclear DNA staining with DAPI are shown in **b, d,** and **f,** respectively. Scale bar = 1 μm.

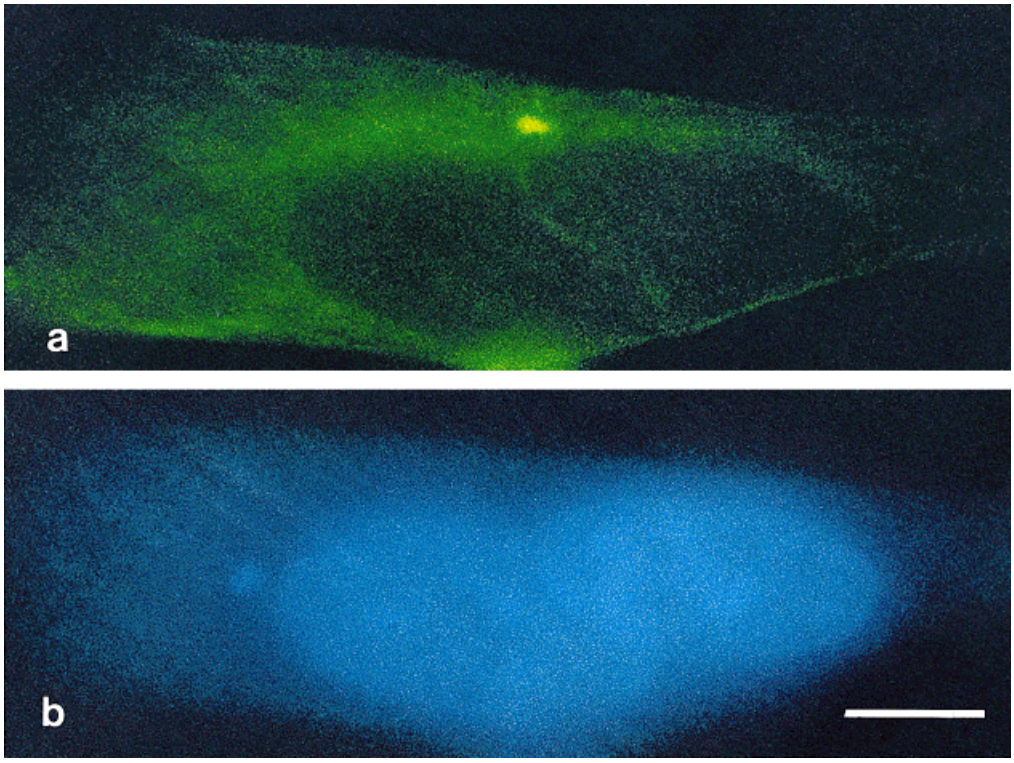

Fig. 6. **a:** Immunofluorescence micrograph of centrosomes in LNCaP cells stained with the human autoimmune antibody SPJ show typical centrosomes closely associated with the nucleus in cells treated with 0.05 nM R1881. **b:** Fluorescence images for DNA in corresponding nuclei. Growth stimulation of LNCaP cells with low concentrations of R1881 (0.05 nM) did not affect centrosome organization (**a,** centrosomes; **b,** DNA). Scale bar = 1 μm.

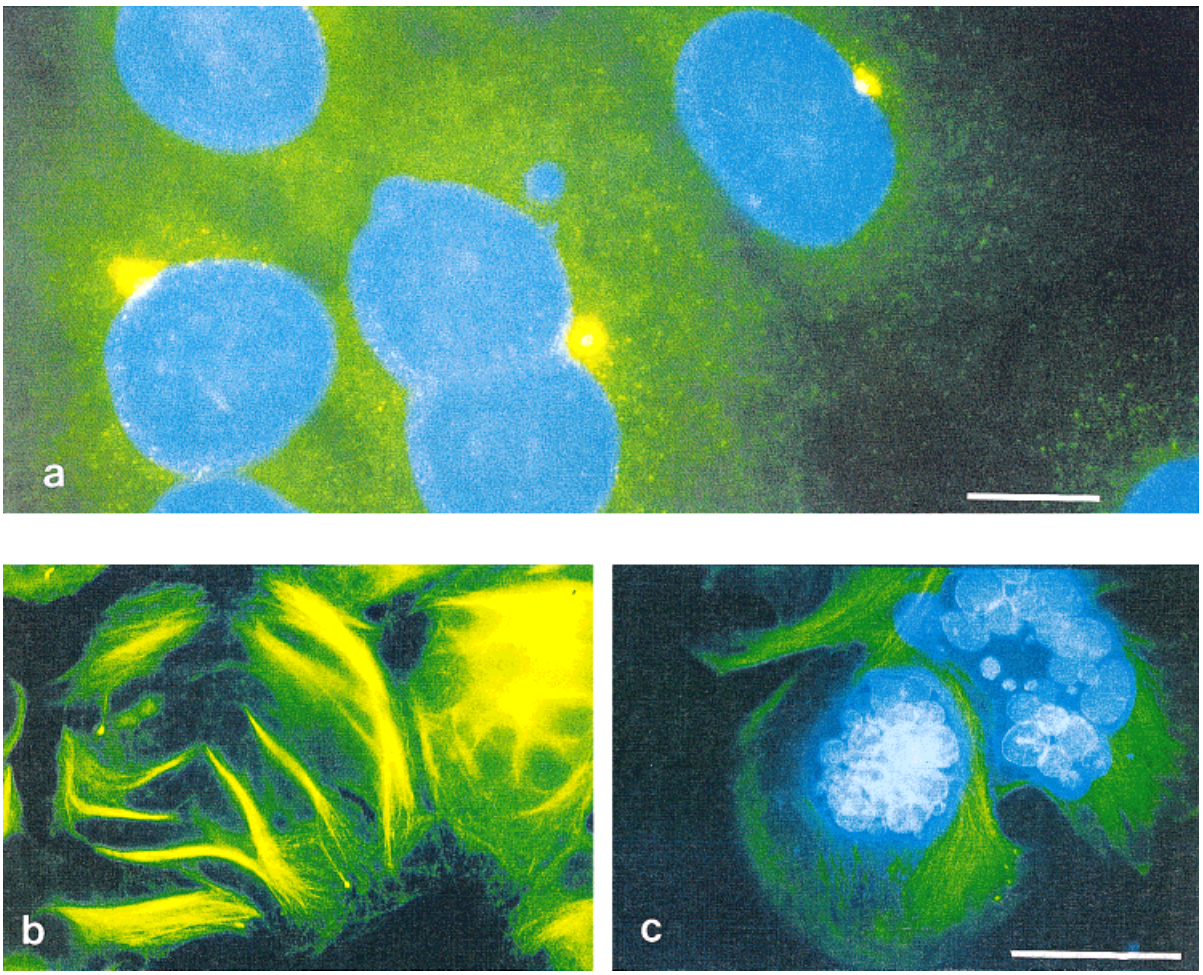

Fig. 7. Immunofluorescence micrographs of control DU145 cells double-stained for centrosomes and DNA (**a**) and of taxol-treated DU145 cells with intensive microtubule bundling after 72 h of taxol treatment (**b**). Micronucleation of DNA in taxol-treated DU 145 cells shown with DAPI staining (**c**). Scale bars = 5 μm.

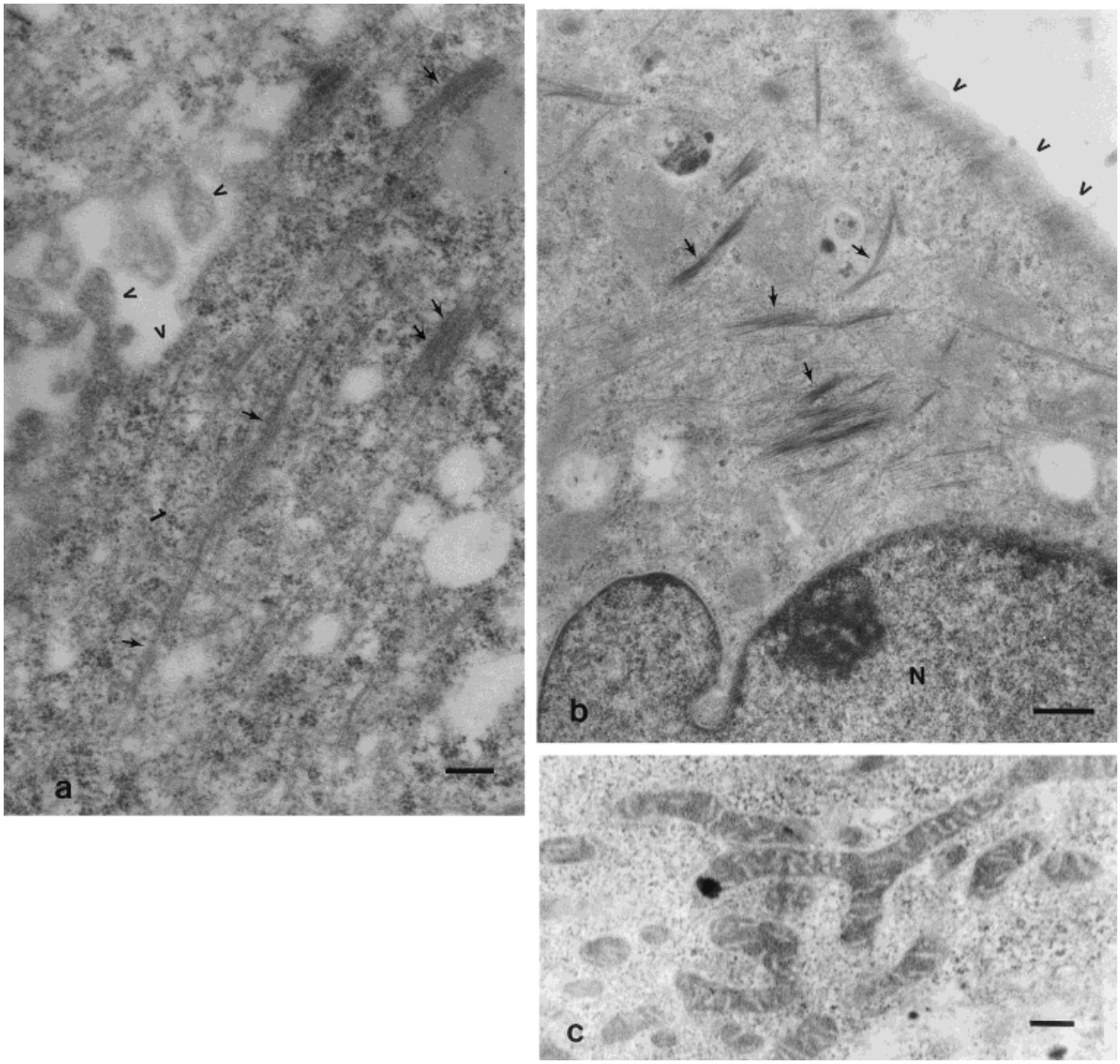

Fig. 8. Transmission electron micrographs of taxol-treated LNCaP (**a**) and DU145 (**b,c**) cells. LNCaP cells (**a**) display long bundles of microtubules (arrows), while extensive bundling of microtubules (arrows) is shown in **b** for DU145 cells. Differences are also noted in the surface of both cell types. While LNCaP cells have cell surfaces with regular microvilli (open arrows) similar to those seen in untreated LNCaP cells, taxol treatment of DU145 cells causes surface alterations (b, open arrows), which are indications for apoptosis. **c:** Morphological mitochondrial alterations in DU145 cells, which are also indications for apoptosis in DU145 cells. Scale bar (a,c) = 200 nm. Scale bar (b) = 500 nm.

gen (0.05 nM) corresponding to levels after age 40 stimulated cell growth. Taxol did not have additional effects in LNCaP cells up until 72 h but induced micronucleation of DNA in androgen-independent DU145 cells. The experiments presented also show that mitochondria are altered in 1 nM R1881 hormone-treated LNCaP cells, related to increased oxidative stress associated with high hormone levels [Ripple et al., 1999]. The concentrations of R1881 used in our experiments show the described effects under our culture conditions [Ripple et al., 1997a,b, 1999]. Other investigators have used different culture conditions and obtained different dose-dependent effects [Lu et al., 1997]. The different results obtained by different investigators are related to the concentration of androgen in which the cells are maintained, to the concentration of serum in which the experiment is conducted, and on the type of LNCaP cells [Ripple et al., 1997b]. In our hands, 0.05 nM R1881 will consistently stimulate cell growth, while we

consistently see growth inhibition with 1 nM R1881 under our culture conditions [Ripple et al., 1999]. We calculated that 1 nM R1881 corresponds to physiological concentrations of testosterone and DHT in human serum of adults of about 3–30 ng/ml, corresponding to 10–100 nM DHT. Because R1881 is about 10 times more potent than DHT, we used 1 nM R1881 in our experiments as the dose corresponding to physiological conditions [Ripple et al., 1997a,b, 1999].

Hormonal change in prostate tissue in men past age 40 is one of the triggers that can induce abnormal cell divisions and cancer [Wilding, 1995]. While this knowledge has been used to design treatments including hormone withdrawal, the side effects are severe and can result in osteoporosis, among other diseases. New treatments are needed to achieve efficient arrest of prostate tumor growth. Targeting the cytoskeleton in cancer cells has proved a promising avenue for inhibiting malignant cell growth. The cytoskeletal drug taxol has offered hope because it arrests cells at G_2/M of the cell cycle. Taxol inhibits microtubule function by preventing microtubule depolymerization [Schiff and Horwitz, 1980; Schatten et al., 1982], which results in temporary impairment of mitosis and cell division. Until recently, taxol was known only as a cytoskeletal drug, but taxol has been shown to play a role in pathways that favor apoptosis as well [Bhalla, 1998]. Taxol-induced G_2/M arrest is known to trigger the cleavage and activity of caspases, which degrade a number of intracellular substrates, including lamins, retinoblastoma protein, and topoisomerase I, resulting in the morphologic changes and DNA fragmentation of apoptosis.

Taxol has been used as anticancer compound against prostate, ovarian, and metastatic breast cancer and is able to induce intranucleosomal DNA fragmentation and typical morphological features of apoptosis in a number of solid tumor cells. These results indicate that taxol exerts its antitumor effects through secondary mechanisms that may or may not be related to its primary effects on microtubules. It has been shown that taxol-induced microtubular changes and G_2/M arrest are associated with the release of the electron transfer protein cytochrome c from mitochondria into the cytosol. Cytochrome c then binds to APAF-1, which binds, cleaves, and activates caspase-9, ultimately resulting in the cleavage and activity of caspase-3 [Bhalla, 1998]. In our studies, morphological changes of mitochondria were seen in DU145 cells after taxol treatment and showed alterations of mitochondrial cristae. Micronucleation of DNA in DU145 cells is a clear indication of apoptosis after treatment with 10 μM taxol. These morphological features were not seen in LNCaP cells after taxol treatment, indicating that taxol may exert antiproliferative effects on cancer cells through apoptotic pathways that are different for different cell types.

This article also reports the effects of hormones on centrosomes in LNCaP cells treated with 1 nM R1881. The finding that centrosomes become dispersed in the cytoplasm after hormone treatment in LNCaP cells indicates that centrosomes are affected by hormones, which has implications on cell cycle events. The regulation of centrosomes has intrigued investigators since their discovery by Van Beneden and Neyt [1887]. Boveri [1914] proposed that improper centrosome regulation is the origin of malignant tumors. More recently, centrosome abnormalities have been reported in archieved and fresh cancer tissue [Pihan et al., 1998; Lingle et al., 1998; Schatten et al., 1998a,b]. Moreover, it has been shown that overexpression of only one of the numerous centrosome proteins can result in centrosome abnormalities, associated with abnormal cell divisions and cancer [Brinkley and Goepfert, 1998; Pihan et al., 1998]. The finding that centrosomes are affected by hormones might play a role in the development of cancer.

A cascade of well-synchronized events takes place during regular cell cycles that leads to cell division, followed by cellular arrest in most cell systems. Normally, cell division is only required for tissue regeneration, during development of the organism, or during wound healing and tissue repair. Centrosomes and DNA are synthesized during the S phase before the next cell division and are distributed in equal amounts to the daughter cells after division. In normal cells, DNA and centrosomes condense and segregate during mitosis and decondense during the following interphase cycle. The centrosome cycle is typically coordinated with the DNA cycle [Balczon et al., 1995; Balczon, 1996] because centrosomes are required to help obtain precise organization of microtubules, which attach to chromosomes and separate the genomic material into equal parts during cell division. Centrosome disorders can lead to abnormal mitoses and abnormal cell cycle progression, with

attendant consequences for genomic stability [Brinkley and Goepfert, 1998; Lingle et al., 1998; Pihan et al., 1998; Schatten et al., 1998a,b, 1999b; Wiedemeier et al., 1998]. The finding that centrosomes are dispersed in the cytoplasm and dissociated from the nucleus in 1 nM-treated LNCaP cells may either indicate that replication of centrosome proteins has continued in hormone-treated LNCaP cells or that the tightly condensed centrosome material becomes decondensed and loosely aggregated in the cytoplasm. Future studies will determine if centrosome replication continues in hormone-arrested LNCaP cells.

Alteration of centrosome proteins in LNCaP cells treated with high hormone concentrations may be one of the causes of abnormal cell division typically associated with cancer. We recently showed that centrosomes can be chemically altered and form tri- or multipolar mitosis [Schatten and Chakrabarti, 1998; Schatten et al., 1999a]. We report that centrosomes are altered in hormone (1 nM R1881)-treated LNCaP cells, which might play a role during abnormal cell division after age 40, when lower hormone levels favor cell division. The conditions for abnormal divisions might be set up at an earlier age, when hormone levels are still high. The mechanisms that allow dysfunctional centrosomes to organize tri- and multipolar mitotic spindles are not understood. Aside from overexpression of centrosome proteins [Pihan et al., 1998; Lingle et al., 1998], structural defects and folding errors of centrosome material may be involved [Schatten et al., 1986, 1987; Schatten, 1994; Thompson-Coffe et al., 1996]. Abnormal centrosomes are also often detected in aging cells [Schatten et al., 1998c,d], possibly the result of structural defects, of ionic imbalances, or molecular errors during centrosome proliferation [Schatten and Chakrabarti, 1998; Schatten et al., 1988].

Centrosomes are reorganized during the transition from interphase to mitosis, in turn regulated by molecular and ionic controls. Deregulation of centrosome cycles within the cell cycle may contribute to the transformation of normal cells into cancer cells. The reorganization of centrosomes into division-competent cell organelles has been linked to posttranscriptional modifications of nuclear proteins [Petzelt et al., 1997a], to interactions with nuclear matrix proteins [Gueth-Hallonet et al., 1996], to ionic regulation, as well as to calcium and phosphorylation [Vandre et al., 1984; Schatten and Chakrabarti, 1994]. The reorganization of nuclear matrix proteins from the nucleus into mitotic centrosomes may play a role in abnormal function of centrosomes during cancer. Closely associated with the nucleus during interphase, upon entry into mitosis, centrosomes become transformed into an active cell organelle that exhibits structural changes [Joswig and Petzelt, 1990; Joswig et al., 1991; Schatten et al., 1986, 1987, 1992], phosphorylation [Vandre et al., 1984; Schatten and Chakrabarti, 1994], disulfide and sulfhydryl bond formations [Schatten et al., 1993; Schatten, 1994], incorporation of nuclear proteins [Chaly et al., 1984; Tang et al., 1994; Zeng et al., 1994], and posttranscriptional modifications [Petzelt et al., 1997a].

Centrosomes are closely associated with the nucleus during interphase. They are composed of high- and low-molecular weight proteins, some of which are permanently associated with centrosomes such as the microtubule nucleating protein γ-tubulin or the intrinsic centrosome protein centrosomin A [Rothbarth et al., 1993; Petzelt et al., 1997a,b], whereas other centrosome proteins are of nuclear origin such as the nuclear mitotic apparatus protein NuMA [Chaly et al., 1984; Gueth-Hallonet et al., 1996; Zeng et al., 1994; Tang et al., 1994; Gobert and Schatten, 1998]. New centrosome proteins are being discovered [Blomberg-Wirschell et al., 1997; Ohta et al., 1997; Stillwell et al., 1997; Mack et al., 1998], and their structure-function relationships are being explored. Developmental regulation of centrosomal proteins has been reported in plant cells [Hart and Wolniak, 1997] and during fertilization and development in mice [Manandhar et al., 1997a,b]. In these studies, the centrosome proteins centrin and γ-tubulin, respectively, were reported to be developmentally regulated. These findings may also be important for centrosome regulation in cancer. Hormones, which are significant regulators during development, may play a role in centrosome protein expression in cancer.

The studies presented call attention to centrosomes as targets for drug therapy in cancer. Centrosomes are highly specific [Thompson-Coffe et al., 1996] and may even be organ specific [Petzelt et al., 1997a]. Centrosomes are prime targets for controlling cancer growth because they are crucial to cell division and cell proliferation. Centrosomes are composed of a

number of high- and low-molecular-weight proteins that may serve ideal for specific drug targeting. By specifically targeting centrosome proteins, it might be possible to inhibit cell division in cancer without introducing side effects.

ACKNOWLEDGMENTS

It is a pleasure to acknowledge stimulating discussions with Dr. Abe Eisenstark and Dr. Elke Bloh. The Electron Microscopy Core facility is acknowledged for use of the scanning and transmission electron microscopes.

REFERENCES

Balczon R. 1996. The centrosome in animal cells and its functional homologs in plant and yeast cells. Int Rev Cytol 169:25–82.

Balczon R, West K. 1991. The identification of mammalian centrosomal antigens using human autoimmune anticentrosome antisera. Cell Motil Cytoskeleton 20:121–135.

Balczon R, Bao L, Zimmer WE, Brown K, Zinkowski RP, Brinkley BR. 1995. Dissociation of centrosome replication events from DNA synthesis and mitotic division in hydroxyurea-arrested Chinese hamster ovary cells. J Cell Biol 130:105–115.

Bestor T, Schatten G. 1981. Anti-tubulin immunofluorescence microscopy of microtubules present during the pronuclear movements of sea urchin fertilization. Dev Biol 88:80–91.

Bhalla K. 1998. Molecular regulation of taxane-induced apoptosis. Proc Microscopy Society of America 42:1040–1041.

Blomberg-Wirschell M, Young A, Dictenberg J, Purohit A, Doxsey SJ. 1997. Characterization of the centrosome R2. Mol Biol Cell 8:55a.

Boveri T. 1914. Zur Frage der Entstehung maligner Tumoren. Jena, Germany: G. Fisher.

Brinkley BR, Goepfert TM. 1998. Supernumerary centrosomes and cancer: Boveri's hypothesis resurrected. Cell Motil Cytoskeleton 41:281–288.

Bubley GJ, Balk SP. 1996. Treatment of androgen-independent prostate cancer. Oncologist 1:20–35.

Calarco-Gillam PC, Siebert MC, Hubble R, Mitchison T, Kirschner M. 1983. Centrosome development in early mouse embryos as defined by an autoantibody against pericentriolar material. Cell 35:621–629.

Chaly N, Bladon T, Setterfield G, Little JE, Kaplan JG, Brown DL. 1984. Changes in distribution of nuclear matrix antigens during the mitotic cell cycle. J Cell Biol 99:661–671.

Danesi R, Figg WD, Reed E, Myers CE. 1995. Paclitaxel (taxol) inhibits protein isoprenylation and induces apoptosis in PC-3 human prostate cancer cells. Mol Pharmacol 47:1106–1111.

Evans AM, Lestingi TM, Bitran JD. 1998. Intermittent androgen suppression as a treatment for prostate cancer: a review. Oncologist 3:419–423.

Gobert G, Schatten H. 1998. Immunolocalization of nuclear mitotic apparatus (NuMA) protein in MCF-7 breast cancer cells. Mol Biol Cell 9:498.

Gueth-Hallonet C, Weber K, Osborn M. 1996. NuMA: a bipartite nuclear location signal and other functional properties of the tail domain. Exp Cell Res 225:207–218.

Guinan P, Shaw M, Mirochnik Y, Slobodskoy L, Ray V, Rubenstein M. 1998. Paclitaxel is more effective than thalidomide in inhibiting LNCaP tumor growth in a prostate cancer model. Exp Clin Pharmacol 20:739–742.

Hart PE, Wolniak SM. 1997. Developmental regulation of centrin during spermiogenesis in *Marsilea vestita.* Mol Biol Cell 8:56a.

Joswig G, Petzelt C. 1990. The centrosomal cycle: visualization in PtK cells by a monoclonal antibody to centrosomal 32kd protein. Cell Motil Cytoskeleton 15:181–192.

Joswig G, Petzelt C, Werner D. 1991. Murine cDNAs coding for the centrosomal antigen centrosomin A. J Cell Sci 98(Pt1):37–43.

Kane DJ, Sarafian TA, Anton R, Hahn H, Gralla EB, Valentine JS. 1993. Bcl-2 inhibition of neural death: decreased generation of reactive oxygen species. Science 262:1247–1277.

Kreis W, Budman DR, Fetten J, Gonzales AL, Barile B, Vinciguerra V. 1999. Phase I trial of the combination of daily estramustine phosphate and intermittent docetaxel in patients with metastatic hormone refractory prostate carcinoma. Ann Oncol 10:33–38.

Lingle WL, Lutz WH, Ingle JN, Maihle NJ, Salisbury JL. 1998. Centrosome hypertrophy in human breast tumors: implications for genomic stability and cell polarity. Proc Natl Acad Sci USA 95:2950–2955.

Lokeshwar BL. 1999. MMP inhibition in prostate cancer. Ann NY Acad Sci 878:271–289.

Lu S, Tsai SY, Tsai MJ. 1997. Regulation of androgen-dependent prostatic cancer growth: androgen reguklation of CDK2, CDK5, and CKIp16 genes. Cancer Res 57:4511–4516.

Mack GJ, Rees J, Sandblom O, Balczon R, Fritzler MJ, Rattner JB. 1998. Autoantibodies to a group of centrosomal proteins in human autoimmune sera reactive within the centrosome. Arthritis Rheum 41:551–556.

Manandhar G, Joshi HC, Stearns T, Schatten G. 1997a. Centrosome reduction during mouse spermiogenesis—centriole and γ-tubulin degeneration. Mol Biol Cell 8:56a.

Manandhar G, Simerly C, Salisbury JL, Schatten G. 1997b. Centrosome reduction during mouse spermiogenesis—centriole and centrin degeneration. Mol Biol Cell 8:56a.

Narayan P. 1995. Neoplasms of the prostate gland. In: Smith's General Urology. EA Tanaglio and JW McAninch, editors. Norwich, CT: Appleton & Lange. p 392–433.

Oakley CD, Oakley BR. 1989. Identification of γ-tubulin, a new member of the tubulin superfamily encoded by mipA gene of *Aspergillus nidulans.* Nature 338:662–664.

Ohta T, Essner R, Ryu J-H, Palazzo R, Kuriyama R. 1997. Identification and characterization of CEP135, a novel centrosomal component present in a wide range of organisms. Mol Biol Cell 8:57a.

Petrylak DP, Macarthur RB, O'Connor J, Shelton G, Judge T, Balog J, Pfaff C, Bagliella E, Heitjan D, Fine R, Zuech N, Sawczuk I, Benson M, Olsson CA. 1999. Phase I trial of docetaxel with estramustine in androgen-independent prostate cancer. J Clin Oncol 17:958–967.

Petzelt C, Joswig G, Mincheva A, Lichter P, Stammer H, Werner D. 1997a. The centrosomal protein centrosomin A and the nuclear protein centrosomin B derive from one gene by post-transcriptional processes involving RNA editing. J Cell Sci 110:2573–2578.

Petzelt C, Werner D, Schatten H. 1997b. In vivo-labeling of the centrosome of human primary endothelial cells by transfection with a green fluorescence protein-centrosomin-A-construct. Mol Biol Cell 8:56a.

Pienta KJ, Smith DC. 1997. Paclitaxel, estramustine, and etoposide in the treatment of hormone-refractory prostate cancer. Semin Oncol 24(suppl 15):S15–72–S15–77.

Pihan G, Purohit A, Knecht H, Woda B, Quesenberry P, Doxsey S. 1998. Centrosomes and cancer. Cancer Res 58:3974.

Rago R, Mitchen J, Wilding G. 1990. DNA fluorimetric assay in 96-well tissue culture plates using Hoechst 33258 after cell lysis by freezing in distilled water. Anal Biochem 191:31–34.

Ripple MO, Pickhardt PA, Wilding G. 1997a. Alteration in γ-glutamyl peptidase activity and messenger RNA of human prostate carcinoma cells by androgen. Cancer Res 57:2428–2433.

Ripple MO, Henry WF, Rago RP, Wilding G. 1997b. Prooxidant-antioxidant shift induced by androgen treatment of human prostate carcinoma cells. J Natl Cancer Inst 89:40–48.

Ripple MO, Hagopian K, Oberly TD, Schatten H, Weindruch R. 1999. Androgen-induced oxidative stress in human LNCaP prostate cancer cells is associated with multiple mitochondrial modifications. Antioxidant Redox Signaling 1:71–81.

Ris H. 1985. The cytoplasmic filament system in critical point dried whole mounts and plastic-embedded sections. J Cell Biol 100:1474–1487.

Roth BJ, Yeap BY, Wilding G, Kasimis B, McLeod D, Loehrer PJ. 1993. Taxol in advanced, hormone-refractory carcinoma of the prostate. A phase II trial of the Eastern Cooperative Oncology Group. Cancer 72:2457–2460.

Rothbarth K, Petzelt C, Lu X, Todorov IT, Joswig G, Pepperkok R, Ansorge W, Werner D. 1993. cDNA-derived molecular characteristics and antibodies to a new centrosome-associated and G2/M phase-prevalent protein. J Cell Sci 104(pt 1):19–30.

Schatten G, Schatten H, Bestor T, Balczon R. 1982. Taxol inhibits the nuclear movements during fertilization and induces asters in unfertilized sea urchin eggs. J Cell Biol 94:455–465.

Schatten H. 1994. Dithiothreitol prevents membrane fusion but not centrosome or microtubule organization during the first cell cycles in sea urchins. Cell Motil Cytoskeleton 27:59–68.

Schatten H, Chakrabarti A. 1998. Centrosome structure and function is altered by chloral hydrate and diazepam during the first reproductive cell cycles in sea urchin eggs. Eur J Cell Biol 75:9–20.

Schatten H, Chakrabarti A. 1994. Centrosomes are phosphorylated in sea urchin eggs throughout the cell cycle, during artificial activation and when microtubule growth is inhibited. In: Proceedings of the fifty-second annual meeting of the Microscopy Society of America, San Francisco Press, San Francisco, p 296–297.

Schatten H, Schatten G, Mazia D, Balczon R, Simerly C. 1986. Behavior of centrosomes during fertilization and cell division in mouse oocytes and sea urchin eggs. Proc Natl Acad Sci USA 83:105–109.

Schatten H, Walter M, Mazia D, Biessmann H, Paweletz N, Coffe G, Schatten G. 1987. Centrosome detection in sea urchin eggs with a monoclonal antibody against *Drosophila* intermediate filament proteins: characterization of stages of the division cycle of centrosomes. Proc Natl Acad Sci USA 84:8488–8492.

Schatten H, Walter M, Biessmann H, Schatten G. 1988. Microtubules are required for centrosome expansion and positioning while microfilaments are required for centrosome separation in sea urchin eggs during fertilization and mitosis. Cell Motil Cytoskeleton 11:248–259.

Schatten H, Walter M, Biessmann H, Schatten G. 1992. Activation of maternal centrosomes in unfertilized sea urchin eggs. Cell Motil Cytoskeleton 23:61–70.

Schatten H, Paweletz N, Balczon R. 1993. Sulfhydryl bond formation is a prerequisite for proper cycling of centrosomes and chromosomes in mammalian tissue culture cells. In: Proceedings of the fifty-first annual meeting of the Microscopy Society of America. p 342–343.

Schatten H, Ripple M, Balczon R, Taylor M, Crosser M. 1998a. Centrosome proliferation in the human androgen-responsive LNCaP and the androgen-independent DU145 prostate cancer cell lines. Proc Microscopy Society of America 56:1066–1967.

Schatten H, Ripple M, Balczon R, Taylor M. 1998b. Centrosome abnormalities in cancer cells and tissue. ICEM14. Electron Microsc 4:243–244.

Schatten H, Hedrick J, Chakrabarti A. 1998c. Centrosome abnormalities in cells during aging. Scanning 20:221–222.

Schatten H, Hedrick J, Chakrabarti A. 1998d. The cytoskeleton of *Drosophila* Schneider Line-1 and Kc23 cells undergoes significant changes during long-term culture. Cell Tissue Res 294:525–535.

Schatten H, Hueser C, Chakrabarti A. 1999a. Centrosome structure and function is altered by experimental manipulations with formamide: implications for abnormal cell divisions during cancer. In: Microscopy and Microanalysis 5:1286–1287.

Schatten H, Wiedemeier A, Taylor M, Lubahn D, Greenberg NM, Besch-Williford C, Rosenfeld C, Day K, Ripple M. 1999b. Centrosome and centriole abnormalities during cancer in the transgenic adenocarcinoma mouse prostate (TRAMP) model. In: Microscopy and Microanalysis 5:1152–1153.

Schiff PB, Horwitz SB. 1980. Taxol stabilizes microtubules in mouse fibroblast cells. Proc Natl Acad Sci USA 77:1561–1565.

Smith DC, Pienta KJ. 1999. Paclitaxel in the treatment of hormone-refractory prostate cancer. Semin Oncol 26(1 suppl 2):109–111.

Stearns ME, Wang M. 1992. Taxol blocks processes essential for prostate tumor cell (PC-3 ML) invasion and metastasis. Cancer Res 52:3776–3781.

Stearns T, Kirschner M. 1994. In vitro reconstitution of centrosome assembly and function: the central role of γ-tubulin. Cell 76:623–637.

Stillwell E, Palacios M, Fertig N, Medsgar T, Joshi H. 1997. Mol Biol Cell 8:57a.

Tanagho EA, McAninch JW, editors. 1995. Smith's general urology. E Norwalk, CT: Appleton & Lange.

Tang TK, Tang CJ, Chao CJ, Wu CW. 1994. Nuclear mitotic apparatus protein (NuMA): spindle association, nuclear targeting and differential subcellular localization of various NuMA isoforms. J Cell Sci 107:1389–1402.

Thompson IM, Coltman CA, Brawley OW, Ryan A. 1995. Chemoprevention of prostate cancer. Semin Urol 13:122–129.

Thompson-Coffe C, Coffe G, Schatten H, Mazia D, Schatten G. 1996. Cold-treated centrosome: isolation of centrosomes from mitotic sea urchin eggs, production of an anticentrosomal antibody, and novel ultrastructural imaging. Cell Motil Cytoskeleton 33:197–207.

Tyrrell CJ. 1999. Controversies in the management of advanced prostate cancer. Br J Cancer 79:146–155.

Van Beneden E, Neyt A. 1887. Bull Acad R Belg Ser 3 14.

Vandre D, Davis F, Rao P, Borisy GG. 1984. Phosphoproteins are components of mitotic microtubule organizing centers. Proc Natl Acad Sci USA 81:4439–4443.

Wiedemeier A, Taylor M, Lubahn D, Besch-Williford C, Rosenfeld C, Day K, Schatten H. 1998. Cytoskeletal, centrosome, and nuclear abnormalities are associated with advanced stages of prostate cancer: analysis in the transgenic adenocarcinoma mouse prostate (TRAMP) model. Mol Biol Cell 9:492.

Wilding G. 1995. Endocrine control of prostate cancer. Cancer Surv 14:43–62.

Zeng C, He D, Brinkley BR. 1994. Localization on NuMA protein isoforms in the nuclear matrix of mammalian cells. Cell Motil Cytoskeleton 29:167–176.

Zi X, Agarwal R. 1999. Silibinin decreases prostate-specific antigen with cell growth inhibition via G1 arrest, leading to differentiation of prostate cancer cells: implications for prostate cancer intervention. Proc Natl Acad Sci USA 96:7490–7495.